

## Finite Element Modeling of Calcium Signaling in T-Lymphocytes

H. Kumar<sup>1\*</sup>, K.R. Pardasani<sup>2</sup>

<sup>1\*</sup>Department of Mathematics, Maulana Azad National Institute of Technology, Bhopal, India

<sup>2</sup>Department of Mathematics, Maulana Azad National Institute of Technology, Bhopal, India

Corresponding Author: [hemantkumar2654@gmail.com](mailto:hemantkumar2654@gmail.com)

Available online at [www.isroset.org](http://www.isroset.org)

Received: Feb/26/2016, Revised: Mar/12/2016, Accepted: Mar/28/2016, Published: Apr/30/2016

**Abstract**— T-Lymphocytes are crucial for health and disease as they provide cell-mediated immunity. The elevation of intracellular free calcium concentration is an essential triggering signal involved in activation of T-Lymphocytes by antigen. Various calcium concentration distribution patterns are required by the cell to initiate, sustain and terminate its processes for providing immunity. The regulatory mechanisms involved in T-Lymphocytes are not well understood. In this paper, the mathematical model has been developed to study intracellular calcium distribution in T-Lymphocytes for one dimensional steady and unsteady state. The steady state model incorporates the parameters like diffusion coefficient, source influx, ryanodine receptors and buffers while unsteady state model is proposed to study the effect of SERCA pump and buffers on temporal calcium concentration distribution. The Finite element method has been employed to obtain the solution of the proposed mathematical model. The boundary conditions have been framed using biophysical conditions of the problem. A computer program has been developed in MATLAB 7.10 for the entire problem and numerical results are used to study relationships among concentration, position and time with respect to physiological conditions.

**Keywords**- Finite Element Method, T-Lymphocytes, Buffers, Ryanodine Receptor (RyR), SERCA pump, Diffusion Coefficient, Reaction Diffusion Equations, MATLAB

### I. INTRODUCTION

Calcium ( $\text{Ca}^{2+}$ ) is an important messenger in every cell type. It plays a significant role in a number of cellular processes like muscular contraction, synaptic plasticity, gene expression, cell differentiation and so on [27]. In most cases  $\text{Ca}^{2+}$  has its major signaling function when it is elevated in the cytosolic compartment. From there it can also diffuse into organelles such as mitochondria and the nucleus [27]. The  $\text{Ca}^{2+}$  concentration is tightly regulated inside by various  $\text{Ca}^{2+}$  channels, pumps, exchangers (collectively referred to as transporter), and buffers that determine the proportion of  $\text{Ca}^{2+}$  that is free versus bound. The mechanisms involved in  $\text{Ca}^{2+}$  signaling in the cells of living beings are still not well understood. Thus, there is a need to study the mechanisms involved in  $\text{Ca}^{2+}$  dynamics in various cells of a living body for better understanding of the normal functions of the cells and causes of the diseases.

T cells are no exception in this regard. T-lymphocytes or T cells are a type of lymphocyte (itself a type of white blood cell) that play a central role in cell-mediated immunity [8]. They can be distinguished from other lymphocytes, such as B cells and natural killer cells (NK cells), by the presence of a T-cell receptor (TCR) on the cell surface. They do not have antigen-presenting properties (but rather, requiring B cells or NK cells for its antigen-presenting property). TCRs

are not capable to recognize epitopes (antigen determinant) directly. They only [9] bind epitopes associated with an MHC protein and act primarily against cells that harbor intracellular pathogens. T cells develop in the bone marrow, but in order to mature, they need to migrate to thymus. They are called T cells because they mature in the thymus. There are several subsets of T cells, each with a distinct function. They circulate in the lymph and blood; migrate to the lymph nodes, spleen and Payer's patches. T-cells are essential for human immunity. There are several calcium channels and transporters that play a key role in balancing cytoplasmic calcium levels in T cells. Pathways of calcium homeostasis participate in a number of cellular processes that determine the short and long-term function of T-lymphocytes. Therapeutic strategies are now evolving based on the modulation of T-lymphocyte calcium homeostasis in order to combat immune - mediated disorders [1].

$\text{Ca}^{2+}$  entry across the plasma membrane is the most important  $\text{Ca}^{2+}$  stores for T cell activation [2]. The ion channels that regulate calcium influx from the extracellular space in T cells, either by conducting calcium ions or by modulating the membrane potential that provides driving force for calcium influx [3, 4]. The best characterized calcium channel in T cells is the calcium released-activated calcium (CRAC) channel, which is composed of ORAI and stromal interaction molecule (STIM) proteins [1]. The ORAI proteins and most

prominently ORAI1 are the molecular basis for  $Ca^{2+}$  release-activated calcium (CRAC) channels. CRAC/ORAI1 channels are well defined through their biophysical and pharmacological properties [2].

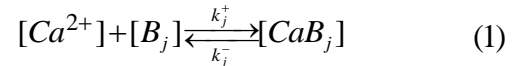
$Ca^{2+}$  dynamics [5] is the exchange of  $Ca^{2+}$  ions between intracellular  $Ca^{2+}$  stores and the cytosol, entering and leaving ions between the cells and binding activity of calcium and calcium binding proteins. The most important calcium binding proteins are itself buffers that are located in  $Ca^{2+}$  stores. The binding of calcium molecules with buffer depends on calcium concentration in the cell [6, 7]. In T-lymphocytes, the main buffer within cytosol is calmodulin (CaM) with 4 calcium binding sites per CaM [1]. There is a diversity of measured CaM concentrations depending on cell type and organ [8]. The concentration dependent binding of  $Ca^{2+}$  to buffers serves as an indicator of the concentration of free calcium concentration in intracellular measurements. Furthermore, other second messengers derived from the adenine dinucleotides, nicotinamide adenine dinucleotide (NAD), and nicotinamide adenine dinucleotide phosphate (NADP) has also been implicated in T-cell calcium signaling [9]. Nicotinic acid adenine dinucleotide phosphate (NAADP) acts as a very early second messenger upon TCR/CD3 engagement, while cyclic ADP-Ribose (cADPR) is mainly involved in sustained partial depletion of the endoplasmic reticulum by stimulating calcium release via ryanodine receptors (RyRs) [1]. It is also important to understand the calcium dynamics in T-lymphocytes, which is possible by studying the temporal calcium distribution in T-lymphocyte cell. The efflux of  $Ca^{2+}$  from the cytosol into the ER plays a crucial role in mediating cytosolic calcium on a temporal scale [21].

A good number of theoretical attempts [12-26] are reported in the literature for the study of calcium signaling in neuron cells, astrocytes, oocytes, acinar cells, fibroblasts, etc. But very few attempts are reported [2, 8, 10] for theoretical studies of calcium signaling in T-lymphocytes. No attempt is reported in the literature for calcium diffusion based study of calcium signaling in T-lymphocytes. The present paper is an attempt to develop the mathematical model for intracellular calcium distribution in the T-lymphocyte cell for one dimensional steady and unsteady state case. The parameters like diffusion coefficient, buffers, source influx and influx of  $Ca^{2+}$  from ryanodine receptor channels are taken in steady state case, while the SERCA pump, source influx and buffers are taken in unsteady state case. The finite element method has been used to obtain the solution. The numerical results are used to study relationships among concentration, position and time with respect to physiological conditions. A computer program has been developed in MATLAB 7.10 for the entire problem and executed on Intel® core™ i3 CPU, 4.00 GB RAM, 2.40 GHz processor.

## II. MATHEMATICAL FORMULATION

### A. Mathematical formulation of Calcium Dynamics

Calcium kinetics in T-lymphocytes are governed by a set of reaction-diffusion equations which can be framed assuming the following bimolecular reaction between  $Ca^{2+}$  and buffer species [6, 19]



Where  $[Ca^{2+}]$ ,  $[B_j]$  and  $[CaB_j]$  represent the cytosolic  $Ca^{2+}$  concentration, free buffer concentration and calcium bound buffer concentration respectively and 'j' is an index over buffer species,  $k_j^+$  and  $k_j^-$  are 'on' and 'off' rates for  $j^{th}$  buffer respectively. Using Fickian diffusion, the buffer reaction diffusion system in one dimension is expressed as [19]

$$\frac{\partial [Ca^{2+}]}{\partial t} = D_{Ca} \nabla^2 [Ca^{2+}] + \sum R_j \quad (2)$$

$$\frac{\partial [B_j]}{\partial t} = D_{B_j} \nabla^2 [B_j] + \sum R_j \quad (3)$$

$$\frac{\partial [CaB_j]}{\partial t} = D_{CaB_j} \nabla^2 [CaB_j] - \sum R_j \quad (4)$$

Where reaction term  $R_j$  is given by

$$R_j = -k_j^+ [Ca^{2+}] [B_j] + k_j^- [CaB_j] \quad (5)$$

$D_{Ca}$ ,  $D_{B_j}$ ,  $D_{CaB_j}$  are diffusion coefficients of free calcium, free buffer and  $Ca^{2+}$  bound buffer respectively and  $\sigma_{Ca}$  is the net influx of  $Ca^{2+}$  from the source. Let  $[B_j]_T = ([B_j] + [CaB_j])$  be the total buffer concentration of  $j^{th}$  buffer and the diffusion coefficient of buffer is not affected by the binding of calcium i.e.,  $D_{B_j} = D_{CaB_j}$ . The equation (5) can be written as [19]

$$R_j = -k_j^+ [Ca^{2+}] [B_j] + k_j^- ([B_j]_T - [B_j]) \quad (6)$$

It is assumed that the buffer concentration is present in excess inside the cytosol so that the concentration of free buffer is constant in space and time i.e.,  $[B_j] \cong [B_j]_\infty$ . Under this assumption equation (6) is approximated by [22]

$$k_j^+ [Ca^{2+}] [B_j] \approx k_j^- ([B_j]_T - [B_j]_\infty) \quad (7)$$

Where  $[B_j]_\infty = \frac{k_j^- [B_j]_T}{(k_j^- + k_j^+ [Ca^{2+}]_\infty)}$  is the background

buffer concentration. Thus for single mobile buffer species equation (2) can be written as [20]

Thus for single mobile buffer species equation can be written as

$$\frac{\partial [Ca^{2+}]}{\partial t} = D_{Ca} \nabla^2 [Ca^{2+}] - k_j^+ [B_j]_\infty ([Ca^{2+}] - [Ca^{2+}]_\infty) + \sigma_{Ca} \quad (8)$$

Here  $[Ca^{2+}]$  is background calcium concentration. We assume a single point source of  $Ca^{2+}$ ,  $\sigma_{Ca}$  at  $r=0$ ; there are no sources for buffers and buffer concentration is in equilibrium with  $Ca^{2+}$  far from the source and  $\nabla$  is the Laplacian operator i.e.,  $\nabla^2 = \frac{\partial^2}{\partial r^2} + \frac{2}{r} \frac{\partial}{\partial r}$ . The point source of calcium

is assumed at  $r = 0$  and as we move away from the source, the calcium concentration achieves its background value i.e.,  $0.1 \mu M$ . Therefore the boundary conditions are given by

$$\lim_{r \rightarrow 0} \left( 4\pi D_{Ca} r^2 \frac{\partial [Ca^{2+}]}{\partial r} \right) = \sigma \quad (9)$$

$$\lim_{r \rightarrow \infty} [Ca^{2+}] = 0.1 \mu M \quad (10)$$

The initial condition is given by

$$[Ca^{2+}]_{t=0} = 0.1 \mu M \quad (11)$$

Thus the equation (8) along with (9), (10) and (11) form an initial boundary value problem. The method of solution is presented in the next section.

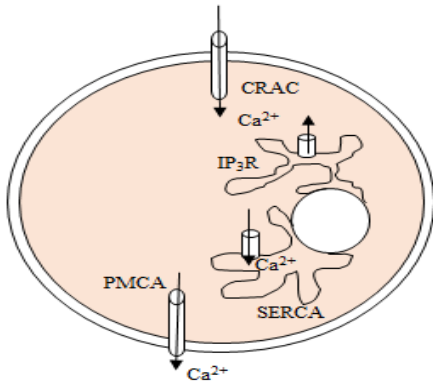


Figure 1 - Scheme of the transmembrane proteins included in the mathematical model [8].

**B. Steady state case**

The mathematical model (8) for a steady state case involving RyR is given by [20]

$$D_{Ca} \nabla^2 [Ca^{2+}] - k_j^+ [B_j]_\infty ([Ca^{2+}] - [Ca^{2+}]_\infty) + \sigma_{RyR} + \delta\sigma(r) = 0 \quad (12)$$

Here  $[Ca^{2+}]$  is background calcium concentration and  $\sigma_{RyR}$  is the influx of calcium through ryanodine receptor channels which is given by [14]

$$\sigma_{RyR} = V_{RyR} P_o ([Ca^{2+}]_{ER} - [Ca^{2+}]) \quad (13)$$

The T-lymphocyte cell is assumed to be spherical in shape [8]. The equations (12) along with (13) for a one dimensional case in polar spherical coordinates is given by

$$\frac{1}{r^2} \frac{\partial}{\partial r} \left( D_{Ca} r^2 \frac{\partial [Ca^{2+}]}{\partial r} \right) - k_j^+ [B_j]_\infty ([Ca^{2+}] - [Ca^{2+}]_\infty) + V_{RyR} P_o ([Ca^{2+}]_{ER} - [Ca^{2+}]) + \delta\sigma(r) = 0 \quad (14)$$

The boundary conditions are given by (9) and (10). For our convenience we write 'u' in lieu of  $[Ca^{2+}]$ . Equation (14) with (9) and (10) in the discretized variational form are expressed as

$$I^{(e)} = \frac{1}{2} \int_{r_i}^{r_j} \left[ r^2 \left( \frac{\partial u^{(e)}}{\partial r} \right)^2 + \alpha r^2 (u^{(e)})^2 - 2\beta r^2 u^{(e)} \right] dr + \psi^{(e)} \left( \frac{\sigma u^{(e)}}{4\pi D_{Ca}} \right)_{r=0} \quad (15)$$

Where  $\alpha = \frac{1}{D_{Ca}} (k_j^+ [B_j]_\infty + V_{RyR} P_o)$ ,

$\beta = \frac{1}{D_{Ca}} (V_{RyR} P_o u_{ER} + k_j^+ [B_j]_\infty u_\infty)$ ,  $\psi^{(e)} = 1$  for  $e = 1$  and

$\psi^{(e)} = 0$  for rest of the elements where  $e = 1, 2, 3, \dots, 50$ .

The shape function of concentration variation within each element is defined as:

$$u^{(e)} = c_1^{(e)} + c_2^{(e)} r \quad (16)$$

Or  $u^{(e)} = p^T c^{(e)}$  (17)

Where  $p^T = [1 \quad r]$  (18)

And  $c^{(e)T} = [c_1^{(e)} \quad c_2^{(e)}]$  (19)

Substituting nodal conditions in equation (17), we get

$$\bar{u}^{(e)} = P^{(e)} * c^{(e)} \quad (20)$$

Where  $\bar{u}^{(e)} = \begin{bmatrix} u_i \\ u_j \end{bmatrix}$  (21)

$$P^{(e)} = \begin{bmatrix} 1 & r_i \\ 1 & r_j \end{bmatrix} \quad (22)$$

From the equation (19), we have

$$c^{(e)} = R^{(e)} * \bar{u}^{(e)} \quad (23)$$

Where  $R^{(e)} = P^{(e)-1}$  (24)

Substituting  $c^{(e)}$  from equation (23) in (17), we get

$$u^{(e)} = p^T R^{(e)} \bar{u}^{(e)} \quad (25)$$

Now the integral  $I^{(e)}$  can be written in the form

$$I^{(e)} = I_l^{(e)} + I_m^{(e)} - I_n^{(e)} + I_k^{(e)} \quad (26)$$

Where  $I_l^{(e)} = \frac{1}{2} \int_{r_i}^{r_j} r^2 \left( \frac{\partial u^{(e)}}{\partial r} \right)^2 dr$  (27)

$$I_m^{(e)} = \frac{1}{2} \int_{r_i}^{r_j} \alpha r^2 (u^{(e)})^2 dr \quad (28)$$

$$I_n^{(e)} = \int_{r_i}^{r_j} \beta r^2 u^{(e)} dr \quad (29)$$

$$I_k^{(e)} = \psi^{(e)} \frac{\sigma}{4\pi D_{Ca}} u^{(e)} \Big|_{r=0} \quad (30)$$

Now we extremize the integral  $I^{(e)}$  w.r.t. each nodal calcium concentration  $u_i$  as given below

$$\frac{dI^{(e)}}{d\bar{u}^{(e)}} = \frac{dI_l^{(e)}}{d\bar{u}^{(e)}} + \frac{dI_m^{(e)}}{d\bar{u}^{(e)}} - \frac{dI_n^{(e)}}{d\bar{u}^{(e)}} + \frac{dI_k^{(e)}}{d\bar{u}^{(e)}} = 0 \quad (31)$$

$$\frac{dI}{d\bar{u}} = \sum \bar{M}^{(e)} \frac{dI^{(e)}}{d\bar{u}} \bar{M}^{(e)T} = 0 \quad (32)$$

Where  $\bar{M}^{(e)} = \begin{bmatrix} 0 & 0 \\ \cdot & \cdot \\ 1 & 0 \\ 0 & 1 \\ \cdot & \cdot \\ 0 & 0 \end{bmatrix}$ ,  $\bar{u} = \begin{bmatrix} u_1 \\ u_2 \\ \cdot \\ \cdot \\ u_{51} \end{bmatrix}$

Assembling the integrals (26), we get

$$I = \sum_{e=1}^{50} I^{(e)} \quad (33)$$

This leads to a following system of linear differential equations

$$[A]_{51 \times 51} [\bar{u}]_{51 \times 1} = [B]_{51 \times 1} \quad (34)$$

Here,  $[\bar{u}] = [u_1 \ u_2 \ u_3 \ \dots \ u_{51}]$ , A is the system matrix and B is the system vector.

C. Unsteady state case

The efflux of  $Ca^{2+}$  from the cytosol into the ER plays a crucial role in mediating cytosolic calcium. The efflux of SERCA pump is given by [23]

$$J_{pump} = K_{pump} [Ca^{2+}] \quad (35)$$

Where  $K_{pump}$  is the maximum pump conductance. Incorporating SERCA pump from equation (35) into the equation (8), we get

$$\frac{\partial [Ca^{2+}]}{\partial t} = D_{Ca} \nabla^2 [Ca^{2+}] - k_j^+ [B_j]_{\infty} ([Ca^{2+}] - [Ca^{2+}]_{\infty}) - K_{pump} [Ca^{2+}] + \sigma_{Ca} \quad (36)$$

The T cell is assumed to be in spherical shape. Therefore equation (36) in polar spherical coordinates for a one dimensional unsteady state case is given by

$$\frac{\partial [Ca^{2+}]}{\partial t} = \frac{1}{r^2} \frac{\partial}{\partial r} \left( D_{Ca} r^2 \frac{\partial [Ca^{2+}]}{\partial r} \right) - k_j^+ [B_j]_{\infty} ([Ca^{2+}] - [Ca^{2+}]_{\infty}) - K_{pump} [Ca^{2+}] + \sigma_{Ca} \quad (37)$$

The same boundary and initial conditions (9), (10) and (11) are imposed and rewritten as

$$[Ca^{2+}]_{r=0} = 0.1 \mu M \quad 0 \leq r \leq \infty \quad (38)$$

Boundary Conditions:

$$\lim_{r \rightarrow 0} (4\pi D_{Ca} r^2 \frac{\partial [Ca^{2+}]}{\partial r}) = \sigma_{Ca} \quad \text{for } t > 0 \quad (39)$$

$$\lim_{r \rightarrow \infty} [Ca^{2+}] = 0.1 \mu M \quad \text{for } t > 0 \quad (40)$$

For our convenience, we write 'u' in lieu of  $[Ca^{2+}]$ . Equation (37) along with (38) to (40) in discretized variational form is expressed as

$$I^{(e)} = \int_{r_i}^{r_j} \left[ \frac{r^2}{2} \left( \frac{\partial u^{(e)}}{\partial r} \right)^2 + \gamma r^2 \left( \frac{(u^{(e)})^2}{2} \right) - \delta r^2 u^{(e)} u_{\infty} + \frac{r^2}{2D_{Ca}} \frac{\partial (u^{(e)})^2}{\partial t} \right] dr$$

$$+ \phi^{(e)} \left( \frac{\sigma_{Ca}}{4\pi D_{Ca}} u^{(e)} \right) \Big|_{r=0} \quad (41)$$

$$I_l^{(e)} = \frac{1}{2} \int_{r_i}^{r_j} r^2 \left( \frac{\partial u^{(e)}}{\partial r} \right)^2 dr \quad (54)$$

where  $\gamma = \frac{1}{D_{Ca}} (k_j^+ [B_j]_{\infty} + K_{pump}), \delta = \frac{k_j^+ [B_j]_{\infty}}{D_{Ca}}$

Here  $e = 1, 2, 3, \dots, 50$ . The term in the last expression of equation (41),  $\phi^{(e)} = 1$  for  $e = 1$  and  $\phi^{(e)} = 0$  for rest of elements, here  $\phi^{(e)} = 1$  implies the location/elements in which source of calcium is present. The shape function of concentration variation within each element is defined as:

$$u^{(e)} = c_1^{(e)} + c_2^{(e)} r \quad (42)$$

Or  $u^{(e)} = p^T c^{(e)} \quad (43)$

Where  $p^T = [1 \ r] \quad (44)$

$$c^{(e)T} = [c_1^{(e)} \ c_2^{(e)}] \quad (45)$$

Substituting nodal conditions in equation (43), we get  $\bar{u}^{(e)} = P^{(e)} * c^{(e)} \quad (46)$

where  $\bar{u}^{(e)} = \begin{bmatrix} u_i \\ u_j \end{bmatrix} \quad (47)$

$$P^{(e)} = \begin{bmatrix} 1 & r_i \\ 1 & r_j \end{bmatrix} \quad (48)$$

From the equation (46), we have

$$c^{(e)} = R^{(e)} * \bar{u}^{(e)} \quad (49)$$

Where  $R^{(e)} = P^{(e)-1} \quad (50)$

Substituting  $c^{(e)}$  from equation (49) in (43), we get

$$u^{(e)} = p^T R^{(e)} \bar{u}^{(e)} \quad (51)$$

Now the integral  $I^{(e)}$  can be written in the form

$$I^{(e)} = I_l^{(e)} + I_t^{(e)} + I_m^{(e)} - I_n^{(e)} + I_k^{(e)} \quad (52)$$

Where

$$I_t^{(e)} = \frac{1}{2} \frac{d}{dt} \int_{r_i}^{r_j} r^2 \left[ \frac{(u^{(e)})^2}{D_{Ca}} \right] dr \quad (53)$$

$$I_m^{(e)} = \frac{1}{2} \int_{r_i}^{r_j} \gamma r^2 (u^{(e)})^2 dr \quad (55)$$

$$I_n^{(e)} = \int_{r_i}^{r_j} \delta r^2 u^{(e)} u_{\infty} dr \quad (56)$$

$$I_k^{(e)} = \phi^{(e)} \frac{\sigma_{Ca}}{4\pi D_{Ca}} u^{(e)} \Big|_{r=0} \quad (57)$$

Assembling the integrals from (52), we get

$$I = \sum_{e=1}^{50} I^{(e)} \quad (58)$$

Extremizing the integral  $I^{(e)}$  w.r.t. each nodal calcium concentration  $u_i$  as given below

$$\frac{dI^{(e)}}{du^{(e)}} = \frac{d}{dt} \frac{dI_t^{(e)}}{du^{(e)}} + \frac{dI_l^{(e)}}{du^{(e)}} + \frac{dI_m^{(e)}}{du^{(e)}} - \frac{dI_n^{(e)}}{du^{(e)}} + \frac{dI_k^{(e)}}{du^{(e)}} \quad (59)$$

$$\frac{dI}{d\bar{u}} = \sum_{e=1}^{50} \bar{M}^{(e)} \frac{dI^{(e)}}{du^{(e)}} \bar{M}^{(e)T} = 0 \quad (60)$$

Where  $\bar{M}^{(e)} = \begin{bmatrix} 0 & 0 \\ \cdot & \cdot \\ 1 & 0 \\ 0 & 1 \\ \cdot & \cdot \\ 0 & 0 \end{bmatrix}$   $\bar{u} = \begin{bmatrix} u_1 \\ u_2 \\ \cdot \\ \cdot \\ u_{51} \end{bmatrix}$

This leads to a following system of linear differential equations.

$$[E]_{51 \times 51} \left[ \frac{\partial \bar{u}}{\partial t} \right] + [F]_{51 \times 51} [\bar{u}]_{51 \times 1} = [G]_{51 \times 1} \quad (61)$$

Where  $E$  and  $F$  are system matrices and  $G$  is system vector. The Crank-Nicolson method is employed to solve the system of equation (61). The time step is taken by us is 0.001 sec. A computer program in MATLAB 7.10 is developed to find numerical solution to the entire problem.

The numerical values of biophysical parameters used in the above models are as stated in the Table-I.

TABLES I. VALUES OF BIOPHYSICAL PARAMETERS

Symbol	Parameter	Value
$D_{Ca}$	Diffusion Coefficient	$250 \mu m / sec^2$
$k_j^+$	On rate for EGTA	$3 / \mu M \text{ sec}$
$k_j^-$	Off rate for EGTA	$1/sec$
$k_j^+$	On rate for BAPTA	$100 / \mu M$
$k_j^-$	Off rate for BAPTA	$10 / sec$
$[B]_\infty$	Total Buffer Concentration	$100 \mu M$
$\sigma$	Source Amplitude	$1 pA$
$V_{RyR}$	RyR Receptor Rate	$0.5 \mu M / sec$
$[Ca^{2+}]_{ER}$	Calcium Concentration of ER	$400 \mu M$
$P_o$	Rate of Calcium Efflux	$0.5 M / sec$
$K_{pump}$	Maximum pump conductance	$20 / sec$

III. RESULTS AND DISCUSSION

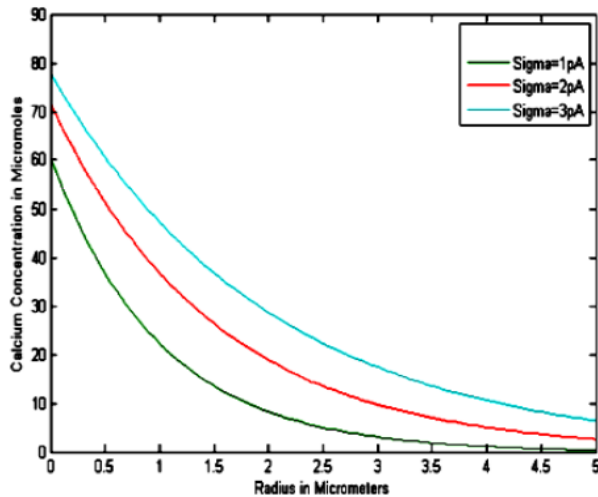


Figure 2 - Radial variation of Calcium concentration for different Source Amplitudes i.e.,  $\sigma = 1 pA, 2 pA, 3 pA, B=25 \mu M$ .

Fig.2 shows radial calcium concentration for different source amplitudes and  $B = 25 \mu M$ . The calcium concentration is maximum at  $r = 0 \mu m$  i.e., source and it decreases as we go

away from the source up to  $r = 5 \mu m$ . It is observed that the calcium concentration is higher for higher values of source amplitudes.

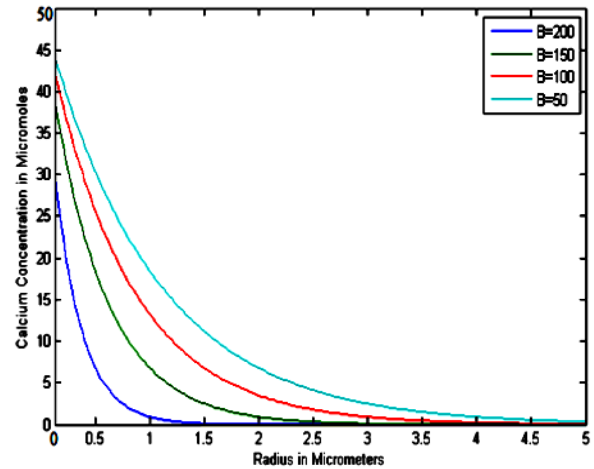


Figure 3 - Radial variation of Calcium concentration for  $\sigma = 1 pA$  four different concentrations of BAPTA buffer i.e,  $B = 50 \mu M, 100 \mu M, 150 \mu M, 200 \mu M$

Fig.3 shows the radial calcium concentration distribution for  $\sigma = 1 pA$  and different values of BAPTA buffer concentrations  $B = 50 \mu M, 100 \mu M, 150 \mu M$  and  $200 \mu M$ . The calcium concentration is maximum at source, i.e.,  $r = 0$ . The peak value of calcium decreases with the increase in the buffer concentration. The gaps among the curves in Fig. 3 indicate that buffer has a significant effect on the calcium concentration distribution in the cell.

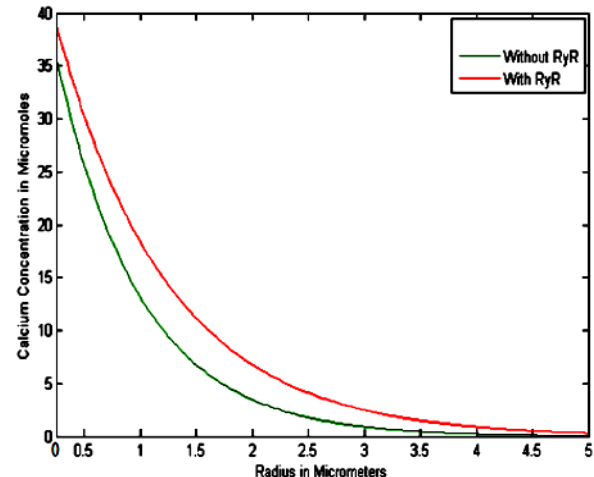


Figure 4 - Radial variation of Calcium concentration for  $\sigma = 1 pA$  in presence and absence of RyR.

Fig.4 shows the radial calcium concentration distribution in the presence and absence of RyR. It is observed that the

presence of RyR raises the peak calcium concentration at the source  $r=0$ . Further the gap between the curves indicates the effect of RyR on calcium concentration distribution in the cell.

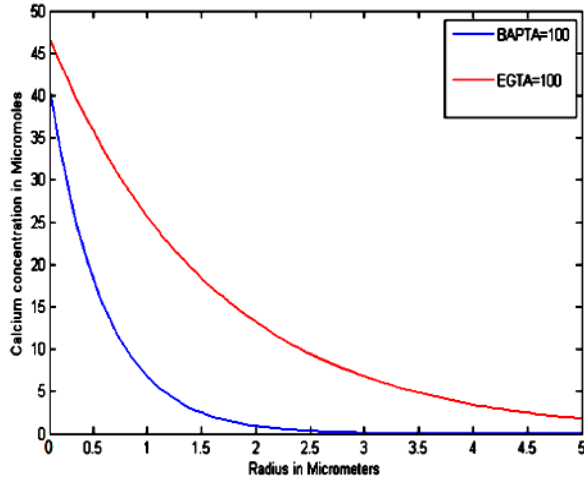


Figure 5 - Radial variation of Calcium concentration for two different types of Buffers EGTA=  $100\mu M$  and BAPTA= $100\mu M$  ,  $\sigma = 1pA$ .

Fig.5 shows the radial calcium concentration distribution due to the two different types of buffers namely BAPTA and EGTA buffers. The fall in the calcium concentration profiles for BAPTA buffer is sharper as compared to that for EGTA buffer. This is because the BAPTA buffer is a fast buffer and binds the calcium ions at a faster rate than the EGTA buffer.

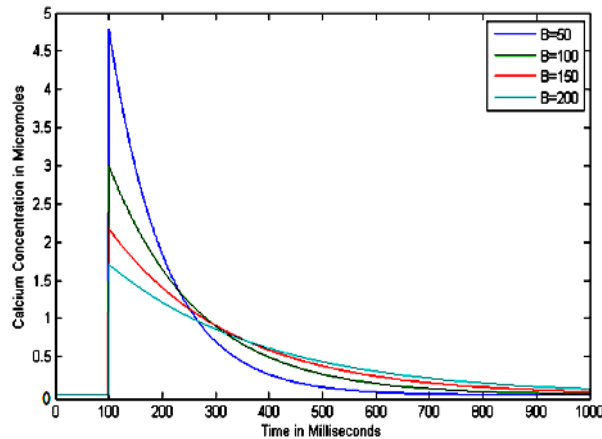


Figure 6 - Temporal variation of calcium concentration in T-lymphocytes for different concentrations of Buffers i.e.,  $B=50\mu M$ ,  $100\mu M$ ,  $150\mu M$ ,  $200\mu M$ .

Fig.6 shows that the temporal variation of  $Ca^{2+}$  concentration in T-lymphocytes for different concentrations of buffer. The

effect of changing the buffer concentration is clear in this figure. We observe that the calcium concentration reaches a steady state in less than 1000 milliseconds. The peak value of  $Ca^{2+}$  concentration is different for different values of buffer concentration. The peak value of  $Ca^{2+}$  concentration is higher in lower concentration of buffer. It is also observed that the steady state is achieved early for higher buffer concentration. The reason for this is that the higher concentration of buffers binds more calcium and then forcing the system to reach steady state early.

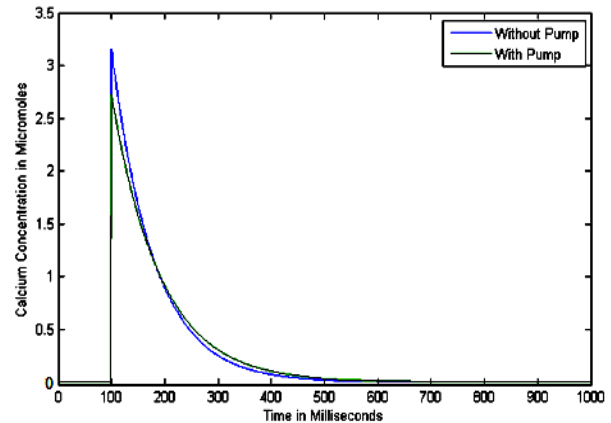


Figure 7 - Temporal variation of calcium concentration in T lymphocytes in the presence and absence of pump.

Fig.7 shows temporal variation of  $Ca^{2+}$  concentration in T-lymphocytes in the presence and absence of SERCA pump. It is observed that  $Ca^{2+}$  concentration is lower in the presence of SERCA pump. The  $Ca^{2+}$  concentration is higher at 100 milliseconds after that it decreases rapidly and becomes almost steady at 600 milliseconds.

The results obtained here are in agreement with biological facts. But no such experimental results are available for comparison at the best of my knowledge. Similar results have been observed in other cells like neuron cells, astrocytes, oocytes etc., [12-26] and our results are in agreement with them.

#### IV. CONCLUSION AND FUTURE SCOPE

The two finite element models were proposed and successfully employed in the present work to study calcium distribution in T-lymphocyte cell. In the first model the effect of RyR and buffers on spatial calcium distribution in T-lymphocyte cell was studied for a one dimensional steady state case. From the results it is concluded that the buffers and RyR have a significant effect on the spatial calcium concentration distribution and thus play an important role in regulating different calcium concentration levels in the cell. In the second model the effect of SERCA pump and buffers on temporal calcium concentration distribution in T-lymphocyte cell. On the basis of results it is concluded that the SERCA pump and Buffers lower down the

calcium concentration to regulate the calcium concentration at the appropriate levels in the cell. In all the cell shows a beautiful coordination among the various components and processes to regulate the calcium concentration levels required for performance of the functions of the cell. Such models can be developed further to get deeper insights of calcium concentration regulation mechanisms in T-lymphocytes and generate the information, which can be of great use in developing protocols for diagnosis and treatment of diseases/disorders caused in T- lymphocytes. In all it is a new research progress in the area of computational cell biology.

There is great scope for development of such models for understanding calcium distribution in T-lymphocytes. The one dimensional models were presented in this thesis. These models can be extended to two and three dimensional studies in order to have more realistic models. The shape of the cell and more details of microstructure can be incorporated in the model for more realistic studies. Different types of influxes and effluxes, can be incorporated to develop more realistic models. The present study was conducted in the normal case. However, it can be extended to the problems involving abnormalities in the structure and processes of the cell leading to various disorders. Thus, there is great scope for developing new models which will be an attention in the area of computational cell biology.

#### ACKNOWLEDGMENT

The first author gratefully acknowledges the financial support given by the Ministry of Human Resource and Development (MHRD), Govt. Of India.

#### REFERENCES

- [1] G. Toldi, "The regulation of Calcium homeostasis in T lymphocytes", *Frontiers in immunology*, Vol.4, pp.1-2, 2013.
- [2] C. Kummerow, C. Junker, K. Kruse, H. Rieger, A. Quintana, M. Hoth, "The immunological synapse controls local and global calcium signals in T lymphocytes", *Immunological reviews*, Vol.231, Issue.1, pp.132-147, 2009.
- [3] M.D. Cahalan, K.G. Chandy, "The functional network of ion channels in T-lymphocytes", *Immunological reviews*, Vol.231, Issue.1, pp.59-87, 2009.
- [4] S. Feske, E.Y. Skolnik, M. Prakriya, "Ion channels and transporters in lymphocyte function and immunity", *Nature Reviews Immunology*, Issue.12, Issue.7, pp.532-47, 2012.
- [5] K. Tsaneva-atanasova, T.J. Shuttleworth, D. I. Yule, J.L. Thompson, J. Sneyd, "Calcium Oscillations and Membrane Transport", *Multiscale Modeling & Simulation*, Vol.3, Issue.2, pp.245-64, 2005.
- [6] E. Neher, "Concentration profiles of intracellular  $Ca^{2+}$  in the presence of diffusible chelators", *Experiment Brain Research*, Vol.14, pp.80-96, 1986.
- [7] Y. Tang, T. Schlumpberger, T. Kim, M. Lueker, R.S. Zucker, "Effects of Mobile Buffers on Facilitation: Experimental and Computational Studies", *Biophysics journal*, Vol.78, pp.2735-2751, 2000.
- [8] C. Schmeitz, E.A. Hernandez-Vargas, R. Fliegert, A.H. Guse and M. M. Hermann, "A mathematical model of T lymphocyte calcium dynamics derived from single transmembrane protein properties", *Frontiers in immunology*, Vol.4, pp.1-16, 2013.
- [9] I.M.A. Ernst, R. Fliegert, A. H. Guse, "Adenine dinucleotide second messengers and T lymphocyte calcium signaling", *Front Immunology*, Vol.4, pp.1-7, 2013.
- [10] P. Hou, R. Zhang, Y. Liu, J. Feng, W. Wang, Y. Wu, J. Ding, "Physiological Role of  $Kv1.3$  Channel in T Lymphocyte Cell Investigated Quantitatively by Kinetic Modeling", *PLOSe One*, Vol.9, Issue.3, pp.1-9, 2014.
- [11] G. D. Smith, "Analytical Steady State Solution to the rapid buffering approximation near an open  $Ca^{2+}$  channel", *Biophysical journal*, Vol.71, Issue.6, pp.3064-3072, 1996.
- [12] S. Tewari and K. R. Pardasani, "Finite Difference Model to Study the effects of  $Na^+$  Influx on Cytosolic  $Ca^{2+}$  Diffusion", *World Academy of Science, Engineering and Technology*, Vol.2, pp.23-34, 2008.
- [13] S. Tewari, K. R. Pardasani, "Finite Element Model to Study Two Dimensional Unsteady State Cytosolic Calcium Diffusion in Presence of Excess Buffers", *IAENG International Journal of Applied Mathematics*, Vol.40, Issue.3, pp.108-112, 2010.
- [14] A. Tripathi, N. Adlakha, "Finite Volume Model to Study Calcium Diffusion in Neuron Involving  $J_{RyR}$ ,  $J_{SERCA}$ , and  $J_{LEAK}$ ", *Journal of Computing*, Vol.3, Issue11, pp.41-46, 2011.
- [15] A. Tripathi, N. Adlakha, "Finite Volume Model to Study Calcium Diffusion In Neuron Cell Under Excess Buffer Approximation", *International J. of Math. Sci & Engg. Appls. (IJMSEA)*, Vol.5, No.3, pp. 437-447, 2011.
- [16] A. Tripathi, N. Adlakha, "Two Dimensional Coaxial Circular Elements in FEM to Study Calcium Diffusion in Neuron Cells", *International Journal of Mathematical Sciences and Engineering Application*, Vol. 6, no. 10, 455-466, 2012.
- [17] B.K. Jha, N. Adlakha, M.N. Mehta, "Finite Volume Model to Study the Effect of Buffer on Cytosolic  $Ca^{2+}$  Advection Diffusion", *International Journal of Engineering and Natural Sciences*, Vol.4, Issue.3, pp.160-163, 2010.
- [18] B.K. Jha, N. Adlakha, M.N. Mehta, "Analytic Solution of Two Dimensional Advection Diffusion Equation Arising In Cytosolic Calcium Concentration Distribution", *International Mathematical Forum* Vol.7, No.3, pp.135-144, 2012.
- [19] P.A. Naik and K.R. Pardasani, "Finite Element Model to Study Radial Calcium Distribution in Oocytes: A one dimensional steady state case study", *International Journal of Advanced Research*, Vol.2, Issue.1, pp.57-66, 2014.
- [20] P.A. Naik, K.R. Pardasani, "Finite Element Model to Study Effect of Buffers in Presence of Voltage Gated  $Ca^{2+}$  Channels on Calcium Distribution in Oocytes for One Dimensional Unsteady State Case", *International Journal of Modern Biology and Medicine*, Vol.4, Issue.3, pp.190-203, 2013.
- [21] P. A. Naik, K. R. Pardasani, "Finite Element Model to Study Effect of  $Na^+/K^+$  pump and  $Na^+/Ca^{2+}$  Exchanger on Calcium Distribution in Oocytes in Presence of Buffers", *Asian Journal of Mathematics and Statistics*, Vol.7, Issue.1, pp.21-28, 2014.
- [22] S. Panday, K.R. Pardasani, "Finite Element Model to Study Effect of Buffers Along With Leak from ER on Cytosolic  $Ca^{2+}$  Distribution in Oocyte", *IOSR Journal of Mathematics (IOSR-JM)* ISSN: 2278-5728, Volume 4, Issue 5, pp. 01-08, 2013.
- [23] S. Panday, K.R. Pardasani, "Finite Element Model to Study Effect of Advection Diffusion and  $Na^+/Ca^{2+}$  Exchanger on  $Ca^{2+}$  Distribution in Oocytes", *Journal of Medical Imaging and Health Informatics*, Vol.52, Issue.1, pp.374-379, 2013.
- [24] S. Panday, K. R. Pardasani, "Finite Element Model to Study the Mechanics of Calcium Regulation in Oocyte", *Journal of Mechanics in Medicine and Biology*, Vol.14, Issue.2, pp.1-16, 2014.



- [25] N. Manhas, J. Sneyd, K.R. Pardasani, “Modelling the transition from simple to complex  $Ca^{2+}$  oscillations in pancreatic acinar cells”, Journal of Biosciences, Vol.39, Issue.3, pp.463-484, 2014.
- [26] M. Kotwani, N. Adlakha, M.N. Mehta, “Numerical Model to Study Calcium Diffusion in Fibroblasts Cell for One Dimensional Unsteady State Case”, Applied Mathematical Sciences, Hikari, Vol.6, Issue.102, pp.5063-5072, 2012.
- [27] M.D. Bootman, P. Lipp, “Calcium Signalling and Regulation of Cell Function”, Encyclopedia of Life Science published by Nature Publishing Group, london, pp.321-347, 2001.

#### AUTHORS PROFILE

Hemant Kumar holds M.Tech. in Computational & Systems Biology from Maulana Azad National Institute of Technology, Bhopal, India. His area of interest is applied mathematics in computational science.



Kamal Raj Pardasani is currently Professor, Department of Mathematics at Maulana Azad National Institute of Technology, Bhopal, India. He holds Ph.D. in Mathematical Biology. His current research areas include Mathematical & Computational Biology, Bioinformatics/ Biocomputing, Data Mining, Modelling and Simulation & Finite Element methods.

